Experimental Neurology xxx (xxxx) xxx–xxx

Contents lists available at ScienceDirect

Experimental Neurology

journal homepage: www.elsevier.com/locate/yexnr

Research Paper

Systemic administration of epothilone D improves functional recovery of walking after rat spinal cord contusion injury

Jörg Ruschel*, Frank Bradke*

German Center for Neurodegenerative Diseases, Sigmund-Freud-Strasse 27, 53127 Bonn, Germany

ARTICLE INFO

Keywords:
Axon regeneration
Axon growth
Scarring
Microtubule stabilization
Epothilone D

ABSTRACT

Central nervous system (CNS) injuries cause permanent impairments of sensorimotor functions as mature neurons fail to regenerate their severed axons. The poor intrinsic growth capacity of adult CNS neurons and the formation of an inhibitory lesion scar are key impediments to axon regeneration. Systemic administration of the microtubule stabilizing agent epothilone B promotes axon regeneration and recovery of motor function by activating the intrinsic axonal growth machinery and by reducing the inhibitory fibrotic lesion scar. Thus, epothilones hold clinical promise as potential therapeutics for spinal cord injury. Here we tested the efficacy of epothilone D, an epothilone B analog with a superior safety profile. By using liquid chromatography and mass spectrometry (LC/MS), we found adequate CNS penetration and distribution of epothilone D after systemic administration, confirming the suitability of the drug for non-invasive CNS treatment. Systemic administration of epothilone D reduced inhibitory fibrotic scarring, promoted regrowth of injured raphespinal fibers and improved walking function after mid-thoracic spinal cord contusion injury in adult rats. These results confirm that systemic administration of epothilones is a valuable therapeutic strategy for CNS regeneration and repair after injury and provides a further advance for potential clinical translation.

1. Introduction

Spinal cord injuries (SCIs) of traumatic or non-traumatic origin commonly disrupt spinal cord axons. Regeneration of these injured axons is prevented by a poor neuron-intrinsic regenerative potential (Blackmore et al., 2012; Canty et al., 2013; Liu et al., 2010; Moore et al., 2009; Park et al., 2008; Tedeschi and Bradke, 2017; Ylera et al., 2009) and by a variety of axon growth inhibitory molecules (Cregg et al., 2014; Filbin, 2003; Garcia-Alias and Fawcett, 2012; Hilton and Bradke, 2017; Schwab, 2004), which are expressed by oligodendrocytes, scar-forming glia and fibroblasts (Anderson et al., 2016; Hellal et al., 2011; Klapka et al., 2005; Pasterkamp et al., 1999; Ruschel et al., 2015). As a result, axons fail to re-innervate their former targets, leaving SCI patients with permanent impairments of sensorimotor functions and lifelong disabilities. To date, no clinically approved, disease modifying treatment for human SCI exists.

Recently, a number of therapeutic strategies to improve functional outcomes in SCI patients have entered clinical trials (Ahuja et al., 2017). However, many of these strategies including epidural stimulation (Harkema et al., 2011), the Rho inhibitor Cethrin (Fehlings et al., 2011), cell-based therapies (Manley et al., 2017) and wound healing matrices (Theodore et al., 2016) require surgical intervention to be efficacious. Thus, although these therapeutic interventions hold great promise to become a first line, clinical treatment for SCI, they have a limited availability for continuous, long-term treatment of human SCI.

Systemic delivery of pro-regenerative, blood-brain barrier permeable compounds have shown encouraging results in promoting spinal cord regeneration in experimental models of SCI (Lang et al., 2015; Ruschel et al., 2015) and have potential for treatment of SCI patients in sub-acute stages and during rehabilitation. Intraperitoneal (i.p.) administration of epothilone B improves functional recovery of walking in spinal cord injured rats by reactivating the intrinsic axon growth machinery and by reducing the inhibitory lesion scar (Ruschel et al., 2015). Epothilones have been tested in cancer clinical trials and have received FDA approval as cancer therapeutics (Goodin et al., 2004). Thus, repurposing epothilones for the treatment of SCI could provide a fast track toward clinical approval (Oprea et al., 2011).

Nevertheless, epothilone B showed significant adverse effects after daily dosing in immune deprived mice even when low doses were applied (Chou et al., 1998). This could have important safety implications for a potential clinical translation into SCI patients, which often exhibit impaired immune function (Popovich and McTigue, 2009). By contrast,

* Correspondence to: J. Ruschel, BioAxone BioSciences Inc., 763E Concord Avenue, Cambridge, MA 02138, USA or F. Bradke, German Center of Neurodegenerative Diseases, Sigmund-Freud-Str. 27, 53127 Bonn, Germany
E-mail addresses: joerg.ruschel@bioaxonebio.com (J. Ruschel), frank.bradke@dzne.de (F. Bradke).

https://doi.org/10.1016/j.expneurol.2017.12.001
Received 10 November 2016; Received in revised form 28 October 2017; Accepted 4 December 2017

daily-dosing of immune deprived mice with comparable doses of desoxy-epothilone B, also referred to as epothilone D, was well-tolerated, even though epothilone D exhibits a similar potency in vitro and in cultured cells (Chou et al., 1998). In addition, epothilone D showed CNS bioavailability and efficacy in rodent models of CNS disease (Brunden et al., 2010) and has been tested in clinical trials for CNS indications (Tsai and Boxer, 2014).

Here we report that systemic and post-injury administration of epothilone D improves functional recovery of hindlimb control in adult rats that underwent a mid-thoracic spinal cord contusion injury. Moreover, epothilone D reduced inhibitory fibrotic scar tissue at the lesion site and restored raphespinal innervation to the lumbar spinal cord. Together, these data suggest that epothilone D could be a promising therapeutic candidate for non-invasive treatment of CNS injuries with a translational perspective.

2. Material & methods

2.1. Animal studies ethical statement

All animal experiments in this study were performed in accordance with the German animal welfare law (TierSchG) and the EU Directive 2010/63/EU for animal experiments. The animals were housed and handled in accordance with good animal practice as defined by the Federation for Laboratory Animal Science Associations (FELASA).

2.2. Pharmacokinetic analysis

Adult, female Sprague-Dawley rats (200–250 g) were injected intraperitoneally (i.p.) with 0.75 mg per kg bodyweight (BW) of epothilone B (Selleck) or epothilone D (Abcam). Both drugs were diluted in 50% DMSO/Saline (1:1 mixture of DMSO and physiological saline at room temperature). Animals were euthanized at 6 h, 1 day, 7 days or 14 days after epothilone B/D injection and blood plasma and spinal cord tissue samples were collected. Spinal cord tissue was extracted and homogenized in PBS (1:1, w/v). Aliquots of homogenates and blood plasma were mixed with 1 volume acetonitrile containing 50 ng/ml diazepam as internal standard and the mixture was centrifuged at 12,000*g*. Aliquots of the resulting supernatants were diluted with deionized water (1:1, v/v) and transferred to autosampler vials for LC-MS analysis. Calibration standards in the range of 0.1–240 ng/ml and quality controls were prepared in the same way as the corresponding unknown samples. The HPLC system consisted of an autosampler and an HPLC pump (Surveyor, Thermo Scientific), connected to a triple quadrupole MS (TSQ Quantum Discovery Max, Thermo Scientific) equipped with an electrospray (ESI) interface (Thermo Fisher Scientific, USA) connected to a PC running the standard software Xcalibur 2.1. The HPLC pump flow rate was set to 600 µl/min and samples were separated on a Kinetex 2.6 µm Phenyl-Hexyl 100 50 × 2.1 mm analytical column with a Security Guard Ultra cartridge UHPLC Phenyl for 2.1 mm ID column (Phenomenex, Germany). Gradient elution was facilitated using acetonitrile/0.1% formic acid as organic phase (A) and 0.1% acetic acid (B): % A = 5 (0–0.1 min), 97 (0.4–1.7 min), 5 (1.8–2.5 min). Full scan mass spectra were acquired in the positive mode using syringe pump infusion to identify the protonated quasi-molecular ions $[M + H]^+$. Auto-tuning was carried out for maximizing ion abundance followed by the identification of characteristic fragment ions using a generic parameter set. Ions with the highest S/N ratio were used to quantify the item in the selected reaction monitoring mode (SRM) and as qualifier, respectively. The limit of quantification (LOQ) was defined as the lowest standard concentration taken for the corresponding calibration curve, i.e. 0.1 ng/ml.

2.3. Spinal cord injury studies

The spinal cord contusion injury was performed at thoracic spinal cord segment 9 using an Infinite Horizon impactor device (Precision Systems) as previously described (Scheff et al., 2003). Adult, female Sprague-Dawley rats (200–250 g) were deeply anesthetized by continuous inhalation of isoflurane (2% isoflurane/oxygen). Laminectomy of the thoracic vertebra 9 was performed to expose the spinal cord. The vertebral column was stabilized with 2 forceps, which fixed the lateral processes of thoracic vertebra 8 and 10. The exposed spinal cord was placed and aligned under the impactor according to the manufacturer's instructions. Finally, an impact of 150 kilodyne (kdyn) was applied to the spinal cord. The impact was controlled and monitored with the device-specific software. Inappropriate force impact curves led to exclusion of the animal from the study. A maximum variation of 10% from the set impact force of 150 kdyn was defined as acceptable range. At day 1 and day 15 after contusion injury, animals received a single i.p. injection of epothilone D (Abcam, 0.75 mg/kg BW, N = 15) or vehicle solution (50% DMSO/sterile saline, N = 17). Bodyweight of injected animals was monitored biweekly. One vehicle and three epothilone D injected animals were excluded from the study either because of irregular force impact curves or because no significant loss of hindlimb function was observed at 2 weeks after SCI (see horizontal ladder test), both of which indicating that the spinal cord impact may not have been appropriate. One vehicle and one epothilone D injected animal were excluded due to a recording error of the force-impact curves.

2.4. Horizontal ladder test

To analyze functional recovery of skilled walking, rats were tested on a foot misplacement device at 2, 4, 6 and 8 weeks after contusion injury. 13 vehicle treated animals and 14 epothilone D treated animals were recorded by video while walking over a 1 m long horizontal ladder, elevated 15 cm above the ground with a regular ladder-step distance of 2 cm. In cases where the animal stopped during the run, the trial was considered unquantifiable and repeated. The first two complete runs per animal were digitally examined frame by frame, the total number of major foot slips in between the ladder rungs were counted and normalized to the total number of steps. Foot slips were considered as ‘major’ when at least two third of the hind paw (complete metatarsus) slipped below the lower edge of the ladder rungs. One vehicle treated animal was excluded from subsequent quantification due to a recording error.

2.5. Immunohistochemistry

Immunohistochemistry was performed as previously described (Ruschel et al., 2015). For tissue fixation, animals were deeply anesthetized with an over dose of a ketamine xylazine mixture (1:2) and subsequently perfused transcardially with 4% paraformaldehyde (PFA) solution (in 0.1 M PBS). The spinal cord was dissected from the vertebral column, post-fixed in 4% PFA solution overnight and then placed in sterile 30% sucrose solution for 48 h. Subsequently, a 1 cm piece of spinal cord containing the lesion site and a caudally adjacent 0.5 cm piece of the lumbar spinal cord were embedded in embedding medium (Thermo Scientific) and frozen on dry ice. 25 µm sagittal sections of the lesion site and 20 µm coronal sections of the lumbar spinal cord were obtained using a cryostat (Leica) and mounted on Superfrost™ plus microscope slides (Thermo Scientific). Sections were quenched with 0.3 M glycine (in TBS) for 30 min and then permeabilized with TBS-TritonX-100 (0.5%) for 30 min at room temperature. Sections were transferred to custom made wet-chambers and blocked with 5% heat-inactivated goat serum (Invitrogen) in TBS-TritonX (0.5%) for 1 h. After blocking, sections were incubated at room temperature with primary antibodies diluted in TBS-TritonX (0.5%). Sagittal sections of the lesion site were incubated overnight with rabbit anti-laminin (1:50; Sigma, Cat# L9393) and monoclonal mouse anti-glial fibrillary acidic protein (GFAP; 1:200; Sigma, Cat# C9295) primary antibodies, while coronal sections of the lumbar spinal cord were incubated for 2 days with rabbit

anti-serotonin primary antibody (5-HT, 1:500; Sigma, Cat# S5545). Subsequently, sections were washed 3 times with TBS-TritonX (0.5%) and then incubated for 3 h at room temperature with corresponding secondary antibodies conjugated to fluorophore Alexa 488 or Alexa 568 (1:400; all Invitrogen), respectively. Finally, sections were washed 3 times with TBS-TritonX (0.5%) and mounted with Fluoromount (Invitrogen).

2.6. Confocal microscopy

Confocal images of spinal cord sagittal and coronal sections were obtained using a Zeiss LSM 700 confocal system in a sequential scanning mode. In order to compare immunofluorescence, standard acquisition parameters including exposure time and image resolution were used for each antibody staining. Quantitative measures in sagittal sections of the lesion site were performed in every 12th consecutive section (300 µm interval), providing a full medio-lateral representation of the spinal cord. Fibrotic scarring was determined by measuring the total amount of laminin immuno-positive pixels using Adobe Photoshop software. Injury size was determined by measuring the area delineated by GFAP-immunolabeling using ImageJ. Quantitative measurements in coronal sections of the lumbar spinal cord were performed in the left and right ventral horn in every 24th consecutive section (480 µm interval, 5 sections per animal). 5-hydroxytryptamine (5-HT)-immunopositive pixels were quantified using Adobe Photoshop as described above, the ratio of the 5-HT-immunopositive area and the total area measured was calculated for each image (2 images per section, 10 images per animal) and averaged for each animal.

2.7. Statistics

All values are expressed as means ± S.E.M. Group means of one parameter were compared by using an unpaired Students *t*-test with two-tailed distribution and unequal variances. Statistical analysis of functional recovery was performed by the Cornell Statistical Consulting Unit. The relative number of major foot slips was modeled using a fitted, linear mixed model with fixed effects of group (vehicle vs. epoD), time-point (number of weeks post-injury), and group vs time-point interaction was used (Warner et al., 2017). A random effect was included to account for the repeated measurements on each animal. *R* statistical software (R Core Team, 2016) with the *lmerTest* package (Kuznetsova et al., 2016) was used to fit the mixed models. The *lsmeans* package was used for post-hoc analyses (Lenth, 2016).

3. Results

3.1. Epothilone D reaches the rat spinal cord after systemic administration

We first examined the CNS bioavailability of epothilone D. In adult mice, epothilone D enters the CNS efficiently after i.p. injection (Brunden et al., 2011, 2010). Using LC-MS we compared the amounts of epothilone D and epothilone B in CNS and plasma of naïve, adult rats (180–200 g) that received a single i.p. dose of either 0.75 mg epothilone B (N = 12) or 0.75 mg epothilone D (N = 12) per kg of animal BW. Spinal cord and plasma samples of 3 animals per group were taken at 6 h, 1 day, 7 days or 14 days after i.p. administration. Mass spectrometry analysis revealed that both drugs were detectable in spinal cord and brain early after injection (Fig. 1A and B). The maximum concentration (C_{Max}) in the spinal cord was 33% higher for epothilone B (21.5 ng/g ± 9.1) than epothilone D (14.3 ng/g ± 3.9), which was reached within 24 h after injection for both drugs (Fig. 1A and Table 1). In addition, epothilone B showed a 4-fold longer spinal cord tissue half-life resulting in approximately 3-fold higher tissue exposure (area under the curve (AUC): 5 µg·h/g) in comparison to epothilone D (AUC: 1.6 µg·h/g) (Table 1). Both drugs showed comparable pharmacokinetic differences with regard to C_{Max}, $t_{1/2}$ and AUC in brain tissue (Fig. 2A and Table 1). Interestingly, we observed a rapid epothilone D plasma elimination with no detectable drug amounts already at 6 h post-injection, while epothilone B plasma exposure was measurable for at least 14 days after i.p. administration (Fig. 1C). These data demonstrate that both epothilone B and D show comparable CNS penetration and distribution, with distinct differences in CNS and plasma elimination.

3.2. Systemic administration of epothilone D promotes functional recovery of skilled walking

Given the comparable CNS penetration, we tested whether systemic administration of epothilone D promotes functional recovery of hindlimb function similarly to epothilone B (Ruschel et al., 2015). Adult rats underwent a 150 kdyn spinal cord contusion injury at thoracic level 9. The recorded impact force and tissue displacement of the experimental spinal cord contusion injuries were indistinguishable between groups (Fig. 2A–B) suggesting comparable injury severity. One day and 15 days after injury, one (control) group of animals (N = 13) was injected i.p. with 1 µl vehicle solution (50% DMSO in Saline) per gram BW and a second group (N = 14) was injected i.p. with 1 µl epothilone D solution (0.75 mg/ml in 50% DMSO/Saline) per gram BW, a dose regimen that was chosen based on our previous study (Ruschel et al., 2015). All animals were tested bi-weekly on the horizontal ladder for a time course of 8 weeks post-injury (wpi) to assess the course of hindlimb function. At 2 weeks post-injury, the percentage of major foot slips were comparable between animals of both groups (vehicle: 36.02% ± 5.3 (2 wpi), epoD: 39.13% ± 3.1) (Fig. 2C and Supplementary Movie S1–S2) suggesting that the controlled contusion injuries produced comparable neurological impairments in both groups. However, over the course of the following 6 weeks, epothilone D treated animals the percentage of foot slips decreased by 27% (27.69% ± 3.37) compared to an only 15% decrease (15.45% ± 4.33) in injured controls. In fact, linear regression analysis revealed that the reduction in foot slip number over time was significantly stronger in the treatment group compared to the control group ($P^* = 0.032$) (Fig. 2C). Post-hoc analysis confirmed that at 8 weeks post-injury, the end of the recovery period, vehicle treated rats (Supplementary Movie S3) showed a significantly higher percentage of major foot slips compared to epothilone D treated animals (Supplementary Movie S4) (20.75% ± 3.6 vs. 11.43% ± 2.7, respectively; $P^* = 0.014$) (Fig. 2C). Taken together, these results demonstrate that systemic administration of epothilone D promotes recovery of hindlimb control in spinal cord contused rats.

3.3. Systemic administration of epothilone D reduces scarring and restores raphespinal innervation

Epothilone B improves functional recovery of walking by reducing inhibitory fibrotic scarring and by promoting raphespinal re-innervation of motor neuron pools in the lumbar spinal cord (Ruschel et al., 2015). We therefore hypothesized that epothilone D would lead to similar biological effects. Eight weeks after contusion injury, animals were perfused transcardially with 4% PFA and the spinal cord injury site as well as the lumbar spinal cord were processed for immunohistological analysis. The lesion site was sectioned sagittally and immunolabeled for laminin, a well-established biomarker for fibrotic scarring in the injured CNS (Hellal et al., 2011), in 13 control and 14 epothilone D treated animals. Even though laminin-positive scar tissue was found in epothilone D treated animals as well as injured controls, the total area of laminin immunolabeling was significantly reduced in the epothilone D group (0.59 mm^2 ± 0.072 versus 0.8 mm^2 ± 0.071; $P^* = 0.043$) (Fig. 3A–B). Total injury size was not affected by epothilone D treatment (9.9 mm^2 ± 0.96 in control group, 10.08 mm^2 ± 2.05 in epothilone D treated group; $P = 0.94$) (Fig. 3C).

We then analyzed raphespinal innervation in coronal sections of the ventral horn in the lumbar spinal cord in 7 control and 8 epothilone D

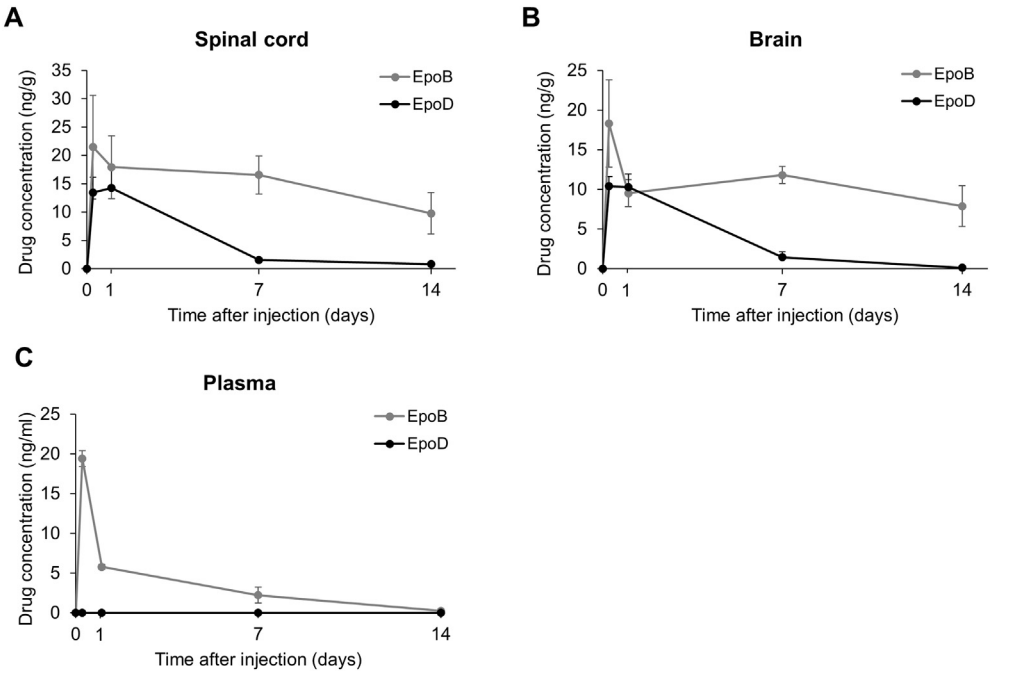

Fig. 1. Epothilone D and epothilone B rapidly distribute into CNS tissue, while both drugs show distinct differences in CNS tissue and plasma exposure and clearance.
Drug levels of epothilone B (EpoB) and epothilone D (EpoD) in rat spinal cord (A), brain (B) and blood plasma (B) after a single i.p. injection of 0.75 mg drug per kg BW. Both, epothilone D and epothilone B rapidly distribute into CNS tissue and measurable drug levels remain in the CNS for at least 7 days (A). By contrast, only epothilone B could be measured in CNS tissue at 14 days post-injection and in blood plasma, while epothilone D is neither detectable in the CNS at 14 days nor at any measured timepoint in the plasma (B). N = 3 animals per group and timepoint. Plotted are mean drug concentration ± S.E.M.

treated animals. Strikingly, the density of serotonin-positive raphespinal fibers was increased by almost 40% in epothilone D treated rats compared to injured controls (3.3% ± 0.6% in control vs. 5.1% ± 0.2% in epothilone D treated animals; $P^* = 0.02$) (Fig. 3D–E). Together, these anatomical analyses reveal that epothilone D treatment reduces fibrotic scarring after SCI and ameliorates raphespinal innervation to the lumbar spinal cord ventral horn.

In summary, the results show that systemic administration of epothilone D improved skilled walking, reduced fibrotic scar tissue and enabled growth of serotonergic axons.

4. Discussion

With regard to clinical translation, an ideal therapeutic strategy for SCI fulfills the following criteria (Kwon et al., 2011): 1) The treatment is available in a form that can be given to humans. 2) It is approved as a clinical therapeutic or, at least, has already been previously tested in human clinical trials for some other related or unrelated conditions. 3) The treatment is neurologically efficient when delivered systemically and when given at post-injury time-points. 4) The systemic application of the treatment does not cause adverse off-target effects on other organs and is compatible with the complications that accompany human SCI. Epothilone B has been tested in clinical trials (Cheng et al., 2008; Goodin et al., 2004) and improved anatomical and neurological outcomes when applied systemically and post-injury in rodent SCI models (Ruschel et al., 2015). However, the significant adverse effects of epothilone B in immune deprived animals (Chou et al., 1998) is a potential caveat for clinical translation as immune dysfunction is a major complication accompanied with SCI in human patients in particular during the acute post-injury period (Popovich and McTigue, 2009). By contrast, epothilone D was well-tolerated by immune deprived rodents even when high doses were applied (Chou et al., 1998).

Both, epothilone B and D have a similar potency in stabilizing microtubules (Chou et al., 1998) and in promoting neurite outgrowth in cultured neurons (Brizuela et al., 2015; Ruschel et al., 2015). Moreover, our data demonstrate that epothilone D exhibits a similar CNS penetration and distribution as epothilone B. Consequently, systemic epothilone D treatment also reduced fibrotic scarring and promoted raphespinal regrowth, although less efficacious than epothilone B treatment (Ruschel et al., 2015). This result may be explained by the more rapid elimination of epothilone D from the CNS and thus the lower overall CNS exposure. However, with regard to clinical translation, a faster organ and plasma clearance is presumably a desirable feature for a SCI drug, as one complication of SCI is perturbed drug metabolism and elimination (Mestre et al., 2011). Thus, our data suggest that due to its similar efficacy, epothilone D is potentially a safer alternative to epothilone B for the treatment of SCI.

An additional key predictor for the translational success of a drug is a defined mechanism of action (Plenge, 2016). MSAs promote axon regeneration after experimental SCI by reducing fibrotic scarring at the lesion site and by promoting regrowth of injured spinal cord axons (Hellal et al., 2011; Ruschel et al., 2015). In accordance with these findings, our data show that epothilone D reduces the amount of fibrotic scar tissue at the lesion site. The fibrotic lesion scar accumulates axon growth inhibitory molecules including semaphorins and chondroitin sulfate proteoglycans (CSPGs) and therefore poses a major barrier for axon regeneration at the lesion site (Hellal et al., 2011; Kawano et al., 2012; Pasterkamp et al., 1999; Ruschel et al., 2015).

Table 1
Pharmacokinetic parameters of epothilone D (EpoD) and epothilone B (EpoB) in CNS tissue and blood plasma of adult rats after a single i.p. administration of 0.75 mg/kg BW.

	Spinal cord				Brain				Plasma			
	C_{Max} (ng/g)	t_{Max} (h)	AUC (µg·h/g)	$t_{1/2}$ (h)	C_{Max} (ng/g)	t_{Max} (h)	AUC (µg·h/g)	$t_{1/2}$ (h)	C_{Max} (ng/g)	t_{Max} (h)	AUC (µg·h/ml)	$t_{1/2}$ (h)
EpoD	14.3 ± 3.9	24	1.585	75.4	10.4 ± 1.2	6	1.166	52	BLD	BLD	NA	NA
EpoB	21.5 ± 9.1	6	5.05	319.7	18.3 ± 5.5	6	3.443	274	19.43 ± 1	6	0.4	10.3

BLD, below limit of detection.
NA, not applicable.

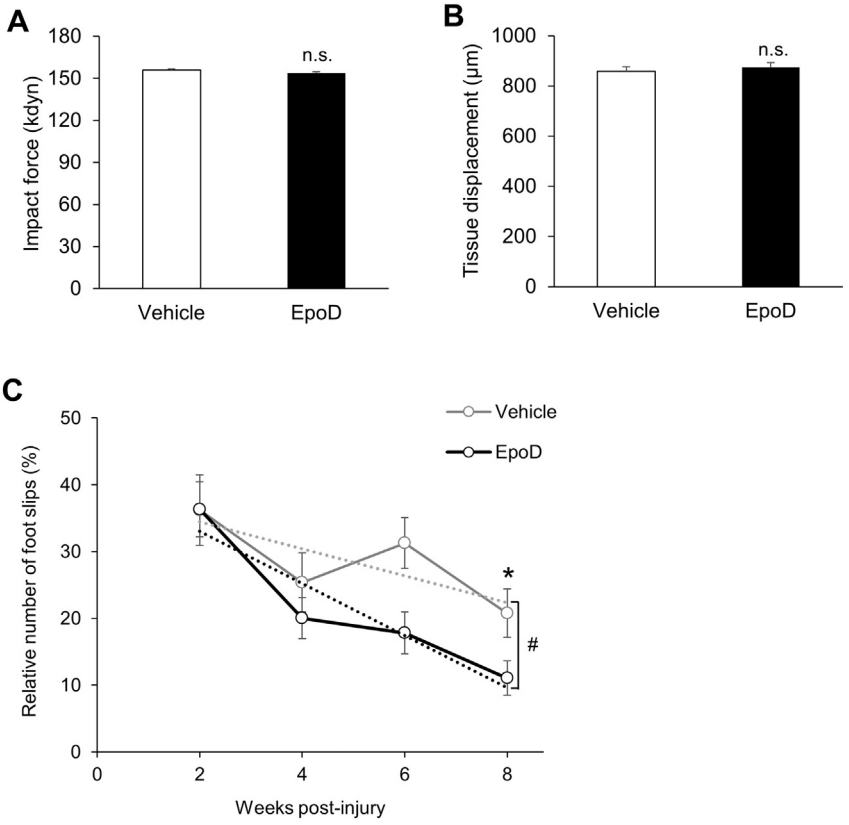

Fig. 2. Systemic administration of epothilone D promotes functional recovery of hindlimb function after spinal cord contusion injury.
Automated recordings of contusion injury parameters revealed indistinguishable impact force (A) and tissue displacement (B) between control and treatment groups, suggesting comparable spinal cord damage in both groups. N = 12–14 animals per group. Plotted are means + S.E.M., $P^* < 0.05$ by Student's *t*-test, n.s. = not significant. Rats traversed over a 1 m long horizontal ladder and the relative number of foot misplacements (foot slips) were used as measurement for recovery of controlled hindlimb movement (C). While both groups showed a reduction of foot slips over time, the decline in relative foot slip number was significantly stronger in epothilone D treated animals (C) as indicated by the linear regression curve (dotted lines, $P^{\#} < 0.05$ by mixed effect linear regression analysis). In addition, at the end of the assessment period, epothilone D treated animals showed significantly fewer foot slips ($P^* < 0.05$ by Student's *t*-test) than uninjured controls. N = 12–14 animals per group. Plotted are mean relative numbers of footfalls + S.E.M. per timepoint and group.

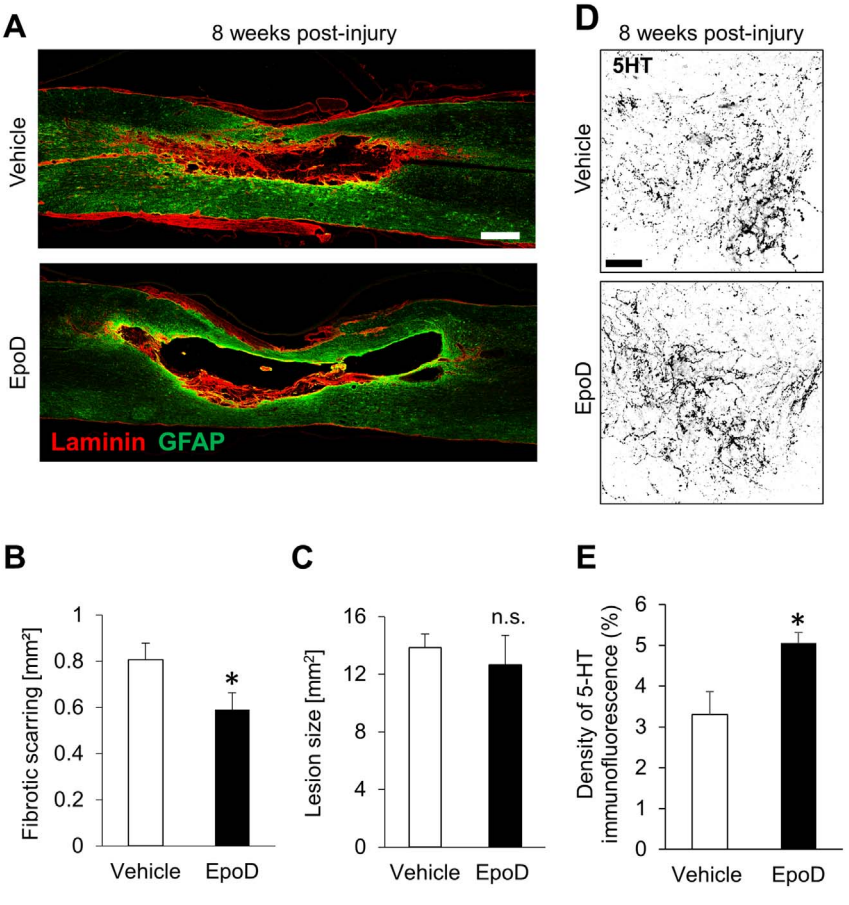

Fig. 3. Systemic administration of epothilone D reduces fibrotic scarring and increases density of raphespinal axons after spinal cord contusion injury.
Eight weeks after contusion injury, sagittal sections of the lesion site were immunolabeled for laminin and for glial fibrillary acidic protein (GFAP) to visualize fibrotic scarring and reactive astrogliosis, respectively (A). Epothilone D treated animals show a reduced amount of laminin immuno-positive scar tissue at the lesion site (A and B) indicating that the treatment reduced fibrotic scarring. Injury size determined by astrogliosis was not affected by the treatment (C). Eight weeks after contusion injury coronal sections of the lumbar spinal cord were immunolabeled for serotonin (5-HT) to visualize raphespinal innervation to the ventral horn (D). 5-HT-density is significantly increased in epothilone D treated animals (D and E), which suggests increased raphespinal innervation of ventral motor neuron pools. N = 13–14 animals for fibrotic scar analysis and 7–8 animals for 5-HT density analysis, respectively. Scale bar = 500 µm in (A) and 200 µm in (D). Plotted are means + S.E.M., $P^* < 0.05$ by Student's *t*-test, n.s. = not significant.

Accordingly, interventions that reduce or at least interfere with fibrotic scarring render the lesion environment more permissive for axon regrowth and regeneration (Hellal et al., 2011; Klapka et al., 2005; Ruschel et al., 2015). In addition, epothilone D enhanced raphespinal density below the injury site (Hellal et al., 2011; Ruschel et al., 2015). It has been shown that promoting regrowth or sprouting of raphespinal axons cause functional recovery of hindlimb function in spinal cord injured rodents (Kaneko et al., 2006; Kim et al., 2004; Ruschel et al., 2015), although a similar relationship between raphespinal innervation and locomotor function remains to be elucidated in humans and non-human primates. As other CNS neurons also show enhanced axon growth using MSAs (Ertürk et al., 2007; Witte et al., 2008; Ruschel et al., 2015) we cannot rule out that different axonal tracts are involved in the functional improvement.

The improvements in walking function after epothilone D treatment are modest and even though the spinal cord contusion injury model used in this study models aspects of human SCI (Hilton et al., 2017; Norenberg et al., 2004), it is considered a moderate injury. Specific walking features such as voluntary and controlled hindlimb locomotion are significantly impaired. It is noteworthy that a substantial number of SCI patients recover walking ability but often remain dependent on walking supports (Scivoletto et al., 2014). Hence, a treatment that ameliorates walking impairments could address an unmet medical need. In addition, the effect of epothilone D in more severe SCI models remains to be investigated.

5. Conclusion

In summary, systemic administration of epothilone D exerts beneficial effects on spinal cord repair and neurological recovery similar to epothilone B. This study suggests that epothilone D might be an interesting alternative to epothilone B for further preclinical development and future clinical translation.

Supplementary data to this article can be found online at https://doi.org/10.1016/j.expneurol.2017.12.001.

Acknowledgments

We thank Daniela Fleischer and Alina Niedzwetzki for their assistance in animal surgery and care. We also thank Michele Curcio, Brett Hilton, Claudia Laskowski, Lisa McKerracher, Katharina Meyer, and Barbara Schaffran, for critical review of the manuscript. We sincerely thank Konstantinos Perrakis and Sach Mukherjee for their input on statistical analysis. We are grateful to Beatrice Sandner, Armin Blesch, Radhika Puttagunta and Norbert Weidner to have tested our findings, which we communicated to them prior to publication in a concerted and independent effort to reproduce the effects of epothilone D on functional and anatomical outcomes after experimental spinal cord injury. This work was supported by IRP and WfL (F.B.).

References

Ahuja, C.S., Nori, S., Tetreault, L., Wilson, J., Kwon, B., Harrop, J., Choi, D., Fehlings, M.G., 2017. Traumatic spinal cord injury—repair and regeneration. Neurosurgery 80, S9–S22.

Anderson, M.A., Burda, J.E., Ren, Y., Ao, Y., O'Shea, T.M., Kawaguchi, R., Coppola, G., Khakh, B.S., Deming, T.J., Sofroniew, M.V., 2016. Astrocyte scar formation aids central nervous system axon regeneration. Nature 532, 195–200.

Blackmore, M.G., Wang, Z., Lerch, J.K., Motti, D., Zhang, Y.P., Shields, C.B., Lee, J.K., Goldberg, J.L., Lemmon, V.P., Bixby, J.L., 2012. Kruppel-like factor 7 engineered for transcriptional activation promotes axon regeneration in the adult corticospinal tract. Proc. Natl. Acad. Sci. U. S. A. 109, 7517–7522.

Brizuela, M., Blizzard, C.A., Chuckowree, J.A., Dawkins, E., Gasperini, R.J., Young, K.M., Dickson, T.C., 2015. The microtubule-stabilizing drug epothilone D increases axonal sprouting following transection injury in vitro. Mol. Cell. Neurosci. 66 (Part B), 129–140.

Brunden, K.R., Zhang, B., Carroll, J., Yao, Y., Potuzak, J.S., Hogan, A.M., Iba, M., James, M.J., Xie, S.X., Ballatore, C., Smith 3rd, A.B., Lee, V.M., Trojanowski, J.Q., 2010. Epothilone D improves microtubule density, axonal integrity, and cognition in a transgenic mouse model of tauopathy. J. Neurosci. 30, 13861–13866.

Brunden, K.R., Yao, Y., Potuzak, J.S., Ferrer, N.I., Ballatore, C., James, M.J., Hogan, A.M., Trojanowski, J.Q., Smith 3rd, A.B., Lee, V.M., 2011. The characterization of microtubule-stabilizing drugs as possible therapeutic agents for Alzheimer's disease and related tauopathies. Pharmacol. Res. 63, 341–351.

Canty, A.J., Huang, L., Jackson, J.S., Little, G.E., Knott, G., Maco, B., De Paola, V., 2013. In-vivo single neuron axotomy triggers axon regeneration to restore synaptic density in specific cortical circuits. Nat. Commun. 4, 2038.

Cheng, K.L., Bradley, T., Budman, D.R., 2008. Novel microtubule-targeting agents - the epothilones. Biologics 2, 789–811.

Chou, T.C., Zhang, X.G., Balog, A., Su, D.S., Meng, D., Savin, K., Bertino, J.R., Danishefsky, S.J., 1998. Desoxyepothilone B: an efficacious microtubule-targeted antitumor agent with a promising in vivo profile relative to epothilone B. Proc. Natl. Acad. Sci. U. S. A. 95, 9642–9647.

Cregg, J.M., DePaul, M.A., Filous, A.R., Lang, B.T., Tran, A., Silver, J., 2014. Functional regeneration beyond the glial scar. Exp. Neurol. 253, 197–207.

Ertürk, A., Hellal, F., Enes, J., Bradke, F., 2007. Disorganized microtubules underlie the formation of retraction bulbs and the failure of axonal regeneration. J. Neurosci. 34, 9169–9180.

Fehlings, M.G., Theodore, N., Harrop, J., Maurais, G., Kuntz, C., Shaffrey, C.I., Kwon, B.K., Chapman, J., Yee, A., Tighe, A., McKerracher, L., 2011. A phase I/IIa clinical trial of a recombinant Rho protein antagonist in acute spinal cord injury. J. Neurotrauma 28, 787–796.

Filbin, M.T., 2003. Myelin-associated inhibitors of axonal regeneration in the adult mammalian CNS. Nat. Rev. Neurosci. 4, 703–713.

Garcia-Alias, G., Fawcett, J.W., 2012. Training and anti-CSPG combination therapy for spinal cord injury. Exp. Neurol. 235, 26–32.

Goodin, S., Kane, M.P., Rubin, E.H., 2004. Epothilones: mechanism of action and biologic activity. J. Clin. Oncol. Off. J. Am. Soc. Clin. Oncol. 22, 2015–2025.

Harkema, S., Gerasimenko, Y., Hodes, J., Burdick, J., Angeli, C., Chen, Y., Ferreira, C., Willhite, A., Rejc, E., Grossman, R.G., Edgerton, V.R., 2011. Effect of epidural stimulation of the lumbosacral spinal cord on voluntary movement, standing, and assisted stepping after motor complete paraplegia: a case study. Lancet 377, 1938–1947.

Hellal, F., Hurtado, A., Ruschel, J., Flynn, K.C., Laskowski, C.J., Umlauf, M., Kapitein, L.C., Strikis, D., Lemmon, V., Bixby, J., Hoogenraad, C.C., Bradke, F., 2011. Microtubule stabilization reduces scarring and causes axon regeneration after spinal cord injury. Science 331, 928–931.

Hilton, B.J., Bradke, F., 2017. Can injured adult CNS axons regenerate by recapitulating development? Development 144, 3417–3429.

Hilton, B.J., Moulson, A.J., Tetzlaff, W., 2017. Neuroprotection and secondary damage following spinal cord injury: concepts and methods. Neurosci. Lett. 652, 3–10.

Kaneko, S., Iwanami, A., Nakamura, M., Kishino, A., Kikuchi, K., Shibata, S., Okano, H.J., Ikegami, T., Moriya, A., Konishi, O., Nakayama, C., Kumagai, K., Kimura, T., Sato, Y., Goshima, Y., Taniguchi, M., Ito, M., He, Z., Toyama, Y., Okano, H., 2006. A selective Sema3A inhibitor enhances regenerative responses and functional recovery of the injured spinal cord. Nat. Med. 12, 1380–1389.

Kawano, H., Kimura-Kuroda, J., Komuta, Y., Yoshioka, N., Li, H.P., Kawamura, K., Li, Y., Raisman, G., 2012. Role of the lesion scar in the response to damage and repair of the central nervous system. Cell Tissue Res. 349, 169–180.

Kim, J.E., Liu, B.P., Park, J.H., Strittmatter, S.M., 2004. Nogo-66 receptor prevents raphespinal and rubrospinal axon regeneration and limits functional recovery from spinal cord injury. Neuron 44, 439–451.

Klapka, N., Hermanns, S., Straten, G., Masanneck, C., Duis, S., Hamers, F.P., Muller, D., Zuschratter, W., Muller, H.W., 2005. Suppression of fibrous scarring in spinal cord injury of rat promotes long-distance regeneration of corticospinal tract axons, rescue of primary motoneurons in somatosensory cortex and significant functional recovery. Eur. J. Neurosci. 22, 3047–3058.

Kuznetsova, A., Brockhoff, P.B., Christensen, R.H.B., 2016. lmerTest: Tests in Linear Mixed Effects Models. R Package Version 2.0-33. URL: https://CRAN.R-project.org/package=lmerTest.

Kwon, B.K., Okon, E., Hillyer, J., Mann, C., Baptiste, D., Weaver, L.C., Fehlings, M.G., Tetzlaff, W., 2011. A systematic review of non-invasive pharmacologic neuroprotective treatments for acute spinal cord injury. J. Neurotrauma 28, 1545–1588.

Lang, B.T., Cregg, J.M., DePaul, M.A., Tran, A.P., Xu, K., Dyck, S.M., Madalena, K.M., Brown, B.P., Weng, Y.L., Li, S., Karimi-Abdolrezaee, S., Busch, S.A., Shen, Y., Silver, J., 2015. Modulation of the proteoglycan receptor PTPsigma promotes recovery after spinal cord injury. Nature 518, 404–408.

Lenth, R.V., 2016. Least-squares means: the R package lsmeans. J. Stat. Softw. 69 (1), 1–33. http://dx.doi.org/10.18637/jss.v069.i01.

Liu, K., Lu, Y., Lee, J.K., Samara, R., Willenberg, R., Sears-Kraxberger, I., Tedeschi, A., Park, K.K., Jin, D., Cai, B., Xu, B., Connolly, L., Steward, O., Zheng, B., He, Z., 2010. PTEN deletion enhances the regenerative ability of adult corticospinal neurons. Nat. Neurosci. 13, 1075–1081.

Manley, N.C., Priest, C.A., Denham, J., Wirth 3rd., E.D., Lebkowski, J.S., 2017. Human embryonic stem cell-derived oligodendrocyte progenitor cells: preclinical efficacy and safety in cervical spinal cord injury. Stem Cells Transl. Med. 10, 1917–1929.

Mestre, H., Alkon, T., Salazar, S., Ibarra, A., 2011. Spinal cord injury sequelae alter drug pharmacokinetics: an overview. Spinal Cord 49, 955–960.

Moore, D.L., Blackmore, M.G., Hu, Y., Kaestner, K.H., Bixby, J.L., Lemmon, V.P., Goldberg, J.L., 2009. KLF family members regulate intrinsic axon regeneration ability. Science 326, 298–301.

Norenberg, M.D., Smith, J., Marcillo, A., 2004. The pathology of human spinal cord injury: defining the problems. J. Neurotrauma 21, 429–440.

Oprea, T.I., Bauman, J.E., Bologa, C.G., Buranda, T., Chigaev, A., Edwards, B.S., Jarvik, J.W., Gresham, H.D., Haynes, M.K., Hjelle, B., Hromas, R., Hudson, L., Mackenzie, D.A., Muller, C.Y., Reed, J.C., Simons, P.C., Smagley, Y., Strouse, J., Surviladze, Z.,

Thompson, T., Ursu, O., Waller, A., Wandinger-Ness, A., Winter, S.S., Wu, Y., Young, S.M., Larson, R.S., Willman, C., Sklar, L.A., 2011. Drug repurposing from an academic perspective. Drug Discov. Today Ther. Strateg. 8, 61–69.

Park, K.K., Liu, K., Hu, Y., Smith, P.D., Wang, C., Cai, B., Xu, B., Connolly, L., Kramvis, I., Sahin, M., He, Z., 2008. Promoting axon regeneration in the adult CNS by modulation of the PTEN/mTOR pathway. Science 322, 963–966.

Pasterkamp, R.J., Giger, R.J., Ruitenberg, M.J., Holtmaat, A.J., De Wit, J., De Winter, F., Verhaagen, J., 1999. Expression of the gene encoding the chemorepellent semaphorin III is induced in the fibroblast component of neural scar tissue formed following injuries of adult but not neonatal CNS. Mol. Cell. Neurosci. 13, 143–166.

Plenge, R.M., 2016. Disciplined approach to drug discovery and early development. Sci. Transl. Med. 8, 349ps315.

Popovich, P., McTigue, D., 2009. Damage control in the nervous system: beware the immune system in spinal cord injury. Nat. Med. 15, 736–737.

R Core Team, 2016. R: A Language and Environment for Statistical Computing. R Foundation for Statistical Computing, Vienna, Austria URL: https://www.R-project.org/.

Ruschel, J., Hellal, F., Flynn, K.C., Dupraz, S., Elliott, D.A., Tedeschi, A., Bates, M., Sliwinski, C., Brook, G., Dobrindt, K., Peitz, M., Brustle, O., Norenberg, M.D., Blesch, A., Weidner, N., Bunge, M.B., Bixby, J.L., Bradke, F., 2015. Axonal regeneration. Systemic administration of epothilone B promotes axon regeneration after spinal cord injury. Science 348, 347–352.

Scheff, S.W., Rabchevsky, A.G., Fugaccia, I., Main, J.A., Lumpp Jr., J.E., 2003. Experimental modeling of spinal cord injury: characterization of a force-defined injury device. J. Neurotrauma 20, 179–193.

Schwab, M.E., 2004. Nogo and axon regeneration. Curr. Opin. Neurobiol. 14, 118–124.

Scivoletto, G., Tamburella, F., Laurenza, L., Torre, M., Molinari, M., 2014. Who is going to walk? A review of the factors influencing walking recovery after spinal cord injury. Front. Hum. Neurosci. 8, 141.

Tedeschi, A., Bradke, F., 2017. Spatial and temporal arrangement of neuronal intrinsic and extrinsic mechanisms controlling axon regeneration. Curr. Opin. Neurobiol. 42, 118–127.

Theodore, N., Hlubek, R., Danielson, J., Neff, K., Vaickus, L., Ulich, T.R., Ropper, A.E., 2016. First human implantation of a bioresorbable polymer scaffold for acute traumatic spinal cord injury: a clinical pilot study for safety and feasibility. Neurosurgery 79, E305–312.

Tsai, R.M., Boxer, A.L., 2014. Clinical trials: past, current, and future for atypical Parkinsonian syndromes. Semin. Neurol. 34, 225–234.

Warner, F.M., Cragg, J.J., Jutzeler, C.R., Röhrich, F., Weidner, N., Saur, M., Maier, D.D., Schuld, C., Curt, A., Kramer, J.K., 2017. Early administration of gabapentinoids improves motor recovery after human spinal cord injury. Cell Rep. 18, 1614–1618.

Witte, H., Neukirchen, D., Bradke, F., 2008. Microtubule stabilization specifies initial neuronal polarization. J. Cell Biol. 180 (3), 619–632.

Ylera, B., Erturk, A., Hellal, F., Nadrigny, F., Hurtado, A., Tahirovic, S., Oudega, M., Kirchhoff, F., Bradke, F., 2009. Chronically CNS-injured adult sensory neurons gain regenerative competence upon a lesion of their peripheral axon. Curr. Biol. 19, 930–936.